Int. J. Electrochem. Sci., 15 **(2020)** 382 – 393, doi: 10.20964/2020.01.08

International Journal of
ELECTROCHEMICAL
SCIENCE
www.electrochemsci.org

Effect of N-N Dimethyltrifluoroacetamide Additive on Low Temperature Performance of Graphite Anode

Wenqing Zuo[1,2,3], *Yongli Cui*[1,2,3,*], *Quanchao Zhuang*[1,2,3], *,Yueli Shi*[1,2,3,] *Pengzhan Ying*[1,2,3,*], *Yanhua Cui*[4]

[1] Li-ion Batteries Lab, School of Materials Science and Engineering, China University of Mining & Technology, Xuzhou 221116, China
[2] The Jiangsu Province Engineering Laboratory of High Efficient Energy Storage Technology and Equipments under grant no. [2017]975-18
[3] The Xuzhou City Key Laboratory of High Efficient Energy Storage Technology and Equipments under grant no. KH17078
[4] Institute of Electronic Engineering China Academy of Engineering Physics,
Mianyang, 621000, P. R. China
[*]E-mail: lilyshuoxu@163.com

Received: 27 May 2019 / *Accepted:* 5 July 2019 / *Published:* 30 November 2019

The effects of N-N Dimethyltrifluoroacetamide (DTA) on the low temperature performance of Li-ion batteries were evaluated, electrolyte ionic conductivity test, charge-discharge, cyclic voltammetry (CV), scanning electron microscope (SEM), X-ray photoelectron spectroscopy (XPS) and electrochemical impedance spectroscopy (EIS) were used to analyze the electrochemical processes. The results showed that the first charge capacities of the graphite electrode in the electrolyte without and with DTA were 72.2 and 114.6mAh g^{-1} at -20°C, 325.1 and 370.8 mAh g^{-1} at 20°C, respectively. After 100 cycles, the corresponding capacities fade to 64.5 and 108.72 mAh g^{-1} at -20°C, 299.5 and 348.5 mAh g^{-1} at 20°C, and the capacity retention were 88.7% and 94.8% at -20°C, 92.12% and 93.9% at 20°C, respectively. The first Coulomb efficiency in the electrolyte with and without DTA was 87.41% and 83.37% at 20°C, respectively. The electrolyte ionic conductivity test shows DTA increases the ionic conductivity of 1mol/L $LiPF_6$ 2:1:4 (vol.%) EC/DEC/EMC. The SEM and XPS showed that DTA additive make the SEI film become more dense and uniform and reduce the content of the unstable substance alkyl lithium carbonate and increase the content of LiF in the SEI film at -20°C. EIS results demonstrated that the SEI resistance of the Li/graphite batteries with DTA was far smaller than those without DTA, especially at -20°C. The improved electrochemical performance with DTA was attributed to the enhancement of the conductivity of the electrolyte, the decrease of the SEI resistance.

Keywords: Lithium-ion batteries; low temperature; N-N Dimethyl Trifluoroacetamide additive; Solid electrolyte interface (SEI) film

1. INTRODUCTION

Nowadays, lithium-ion batteries have become the dominant power source for many portable devices because of their long cycle life and high capacity, such as rechargeable bus, and mobile phone. Its common electrolyte is to dissolve the $LiPF_6$ lithium salt in a carbonate solvent such as ethylene carbonate (EC), iethyl carbonate (DEC), dimethyl carbonate (DMC), and Ethyl ester (EMC), these solvents work stably at room temperature [1]. However, at low temperature, the power performance of lithium-ion batteries deteriorates because the electrolyte solution becomes frozen [2]. Among the commonly used liquid electrolyte carbonate solvents, Polycarbonate (PC) has a low melting point (-49℃) and a high dielectric index [3], which is superior to other solvents at low temperature. Unfortunately, this polymer could lead to surface exfoliation of the graphite anode, which would reduce the reversible capacity [3-5]. The addition of functional additives to the liquid electrolyte is considered to be a promising approach to enhance the performance of lithium-ion batteries for these additives are less usage, low price, and have no side effects [6], and the advantage of additives is that they can stabilize and improve cycle life [7,8], film-forming, protecting the anode or cathode [9-13], and flame retarding [13,14] during cycling. Among the additives, Fluoroethylene carbonate (FEC) has been positively considered as a reaction-type electrolyte additive to modify solid electrolyte interface (SEI) film formed on the graphite anode [6], and it has already prolonged the cycle life of graphite/$LiCoO_2$ cells at room temperature by Rod McMillan [15], and improved the capacity retention of Li/graphite cells at low temperature by Bingxiao Liu [16]. N-N Dimethyl trifluoroacetamide (DTA) and FEC have similar functional groups, and the effect of DTA on the performance of lithium-ion batteries has not been studied so far, especially at low temperature. In this study, DTA was used as an electrolyte additive to explore the electrochemical properties of graphite anodes at low temperature of -20℃.

2. EXPERIMENTAL

Prepa-concentration of graphite electrode: 90 wt% of natural graphite was mixed with 10 wt% polyvinylidene difluoride (PVDF) in N-methyl-2-pyrrolidone as solvent to prepare a slurry. The uniformly mixed slurry was coated on a copper foil and then heated in a vacuum oven at 120℃. The blank electrolyte is 1 mol/L $LiPF_6$ 2:1:4 (vol.%) EC/DEC/EMC solution, and the electrolytes with different concentration of DTA (1 vol.%, 2 vol.% and 3 vol.%) in the above blank solution were prepared in a glove box under a dry argon atmosphere.

In this work, the electrochemical process was analyzed electrolyte ionic conductivity test, charge and discharge test, cyclic voltammetry (CV), electrochemical impedance spectroscopy (EIS), scanning electron microscopy (SEM) and X-ray photoelectron spectroscopy (XPS). The ionic conductivity test of the electrolyte uses the digital metal conductivity tester (FUERTE, Suzhou, China). The coin cells (2025) were assembly in an argon-filled glove box using Cu foil as the cathode, and Celgard 2400 as the diaphragm. The coin cells were galvanostatically charged and discharged in a battery analyzer (LANHE, Wuhan, China) with a high and low temperature test chamber (WD2005, Shanghai Experimental Instrument Factory, China). The CV and EIS of the graphite electrode were tested by a three-electrode system on an electrochemical workstation (CHI660C, Shanghai, China). For the three-electrode system, lithium sheet was used as a counter electrode and a reference electrode. At room temperature（20℃）, the charge and discharge test were performed in the potential range at 0.1-3.0 V with a constant current density of 0.1C (1C = 372 mAh g^{-1}). At low temperature (-20℃), the cells were firstly cycled at a constant current of 0.2C for 5 cycles at 20℃ to form the Solid Electrolyte Interface (SEI) film, and then stayed in -20℃ for 5h to adapt to low temperature environment, then taken charge and discharge cycle at a constant current density of 0.1C. CV was measured at a scan rate of 0.5 mV s^{-1} in the potential range of 0.1-3.0 V. EIS measurements were determined over a frequency range of 10^{-2} to 10^{-5} Hz with an ac voltage signal of ±5mV. After the test was completed, to disassemble the battery in an argon-filled glove box, clean the graphite electrode sheet with DMC, dry the electrode sheet at room temperature, and then characterize the morphology and chemical composition of the electrode sheet using SEM and XPS.

3. RESULTS AND DISCUSSION

3.1. Charge-discharge test

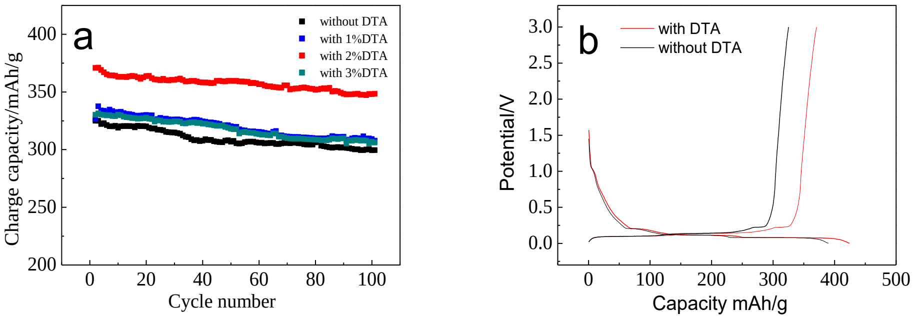

Figure 1. The cyclic performances (a) and the first charge-discharge characteristic (b) of the graphite anode in the electrolyte with different concentration DTA and without additive at 20℃

Figure 1 illustrates the cyclic performances and the first charge-discharge characteristic of the graphite anode in the electrolyte with different concentration DTA and without additive at 20℃. It can be seen in Figure 1a that the DTA additive can improve the specific capacity and cycling performance of graphite anode, and when the volume concentration of DTA additive is 2%, it has attain the best electrochemical performance. At the 100th cycle, the charge capacities with 2 vol. % DTA and without DTA are 348.5 and 299.5 mAh g^{-1}, with 93.90% and 92.12% of the capacity retention concentration as compared with the first cycle. It can be reasonably inferred that the 2 vol. % DTA may be an optimal content additive at the frozen temperature of -20℃. Henceforth, the DTA in the electrolyte refer to the 2 vol. % DTA and for comparison the blank electrolyte is also taken.

It can be seen in Figure 1b the charge and discharge platform of the graphite anode in the electrolyte with and without DTA are similar, a higher small platform at about 0.2 V and a lower larger one at about 0.1V, corresponding to LiC_{18} and LiC_{6-12} reactions, respectively. The first charge and discharge capacities of the graphite electrode in the electrolyte with and without DTA is 424.2 and 370.8 mAh g^{-1}, 390.0 and 325.1 mAh g^{-1}, corresponding to 87.41% and 83.37% of the first coulomb efficiency, respectively, indicating that DTA additive can enhance the charge capacity and initial coulombic efficiency of the graphite electrode at 20°C.

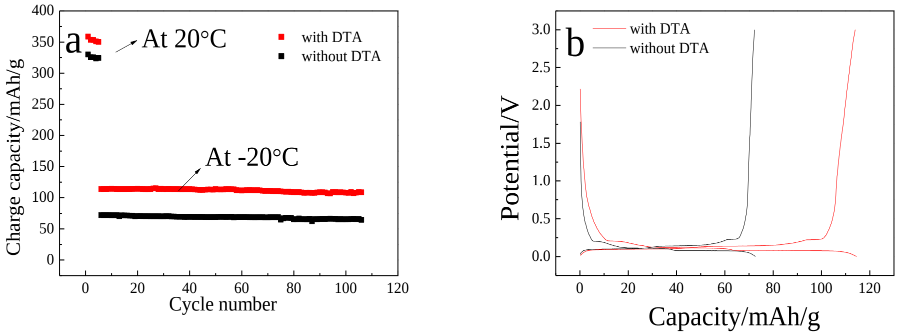

Figure 2. The cyclic performance (a) and the first charge-discharge characteristic (b) of the graphite electrode in the electrolyte with and without DTA at -20°C.

Figure 2 demonstrates the cyclic performances and the first charge-discharge characteristic of graphite electrode in the electrolyte with and without DTA at -20°C. It can be seen that in Figure 2a the sixth charge capacities of the graphite anode with and without DTA at -20°C are 114.0 and 72.2 mAh g^{-1}, after 100 cycles, the corresponding capacities fade to 108.7 and 64.5 mAh g^{-1}, with the capacity retention of 91.8% and 88.7% as compared with the first cycle at -20°C, and 29.67% and 19.54% as compared with the first cycle at 20°C, respectively. It is suggested that the DTA additive can not only enhance dramatically the capacity of the graphite anode, but also increase its long cycle life at low temperature of -20°C.

It is shown that in Figure 2b the charge and discharge platforms of the graphite anode at -20°C are similar to those at 20°C in Figure 1b. The first charge and discharge capacities of the graphite electrodes in the electrolyte with and without DTA at -20°C are 114 and 114.6 mAh g^{-1}, 72.2 and 72.7 mAh g^{-1}.

3.2. CV test

Figure 3 demonstrates the cyclic voltammetries (CVs) of the graphite electrode in the electrolyte with and without DTA at different temperature. It can be seen from Figures 3a and b, the graphite electrode shows three reduction current peaks (peak II, peak III and peak IV) on the first negative potential scan at 20℃. In the next cyclic scan, the peaks II and III of the electrode potential disappeared completely, so the reduction peaks II and III attribute to the solvent molecule EC decomposition and SEI film formation on the surface of the graphite electrode.

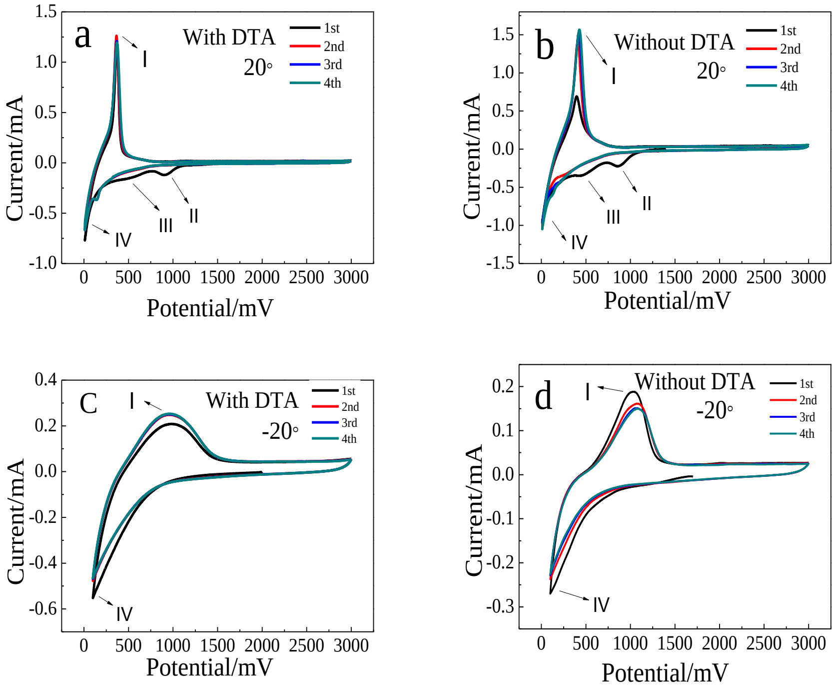

Figure 3. CVs of the graphite electrode in the electrolyte with and without DTA at different temperature (20°C and -20°C).

According to the research of Quanchao Zhuang [9], the process of reductive decomposition of solvent molecules EC mainly contains two processes.

Step one (single-electron reduction process) [17-19]:

$EC + 2e^- + 2Li^+ \rightarrow Li_2CO_3 + C_2H_4$ (1)

Step two (dual electronic reduction process):

$EC + e^- + Li^+ \rightarrow [Li + EC]^-$ (2)

$2\,[Li + EC]^- \rightarrow (-CH_2OCO_2Li)_2 + C_2H_4$ (3)

$2\,[Li + EC]^- \rightarrow (-CH_2CH_2OCO_2Li)_2$ (4)

Therefore, the reduction peak II occurring near 0.9 V can be attributed to the reductive decomposition of EC into lithium carbonate (Li_2CO_3), corresponding to the decomposition reaction 1. The reduction peak III at around 0.6 V can be attributed to the reductive decomposition of EC to form lithium alkyl carbonate ($ROCO_2Li$, R= $-CH_2$,$-CH_2CH_2$...), that is, the dual electronic reduction process of the second step. In addition, a pair of larger redox peaks, the oxidation peak I existing always and the reduction peak IV appearing near 0 V, indicates the reversible extraction/insertion process of lithium ions during cycling.

Compared Figure 3a and b, it is found that the peak III becomes smaller in the electrolyte with DTA, indicating that DTA can inhibit the process of reductive decomposition of EC to form lithium alkyl carbonate, and the content of the unstable substance alkyl lithium carbonate on the SEI film decreases, which would conducive to improve the stability of SEI film. The difference ΔV between the redox peakI/IV in Figures 3a and b is 0.37 and 0.47V, respectively, and the overlap of the curves in Figure 3a is better than that in Figure 3b. This indicates that DTA additive can lower the polarization of the graphite anode and improve its cyclic stable.

In Figure 3c and d the difference ΔV between the peak Iand IV with and without DTA is 0.97 V and 1.1 V at -20°C, respectively, which prove that the hypothermia would drastically cause the polarization of electrode. However, the DTA additive can improve this to a certain degree.

3.3. Electrolyte conductivity test

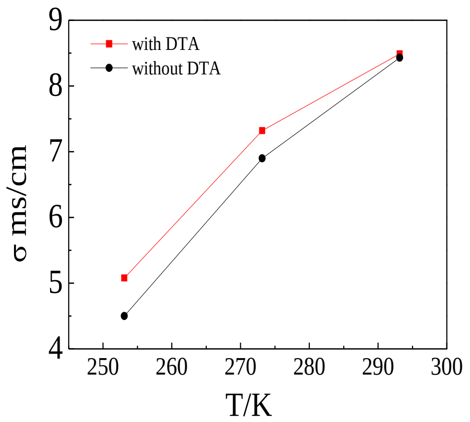

Figure 4. Temperature dependence of conductivity for the electrolytes with and without DTA

Figure 4 exhibits temperature dependence of conductivity for the electrolytes with and without DTA. Obviously, these two systems have very approximate ionic conductivity above 20°C. As the temperature decreases from 20°C to 0 and -20°C, the difference of ionic conductivity between with DTA and without DTA is getting higher and higher, which is attributed to -F group from the DTA additive, a strong electron-withdrawing group [17].

3.4. Characterization of EIS

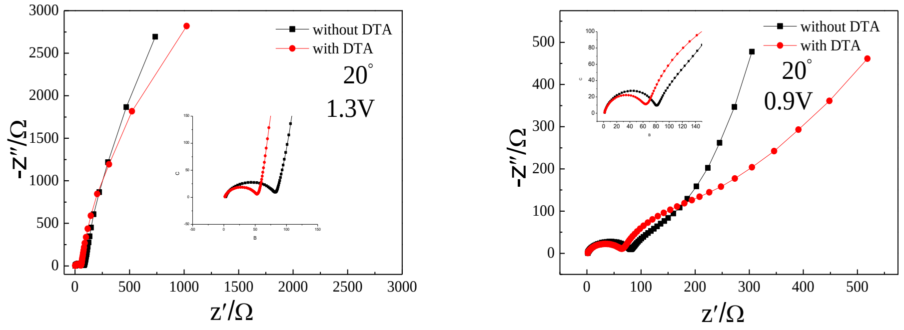

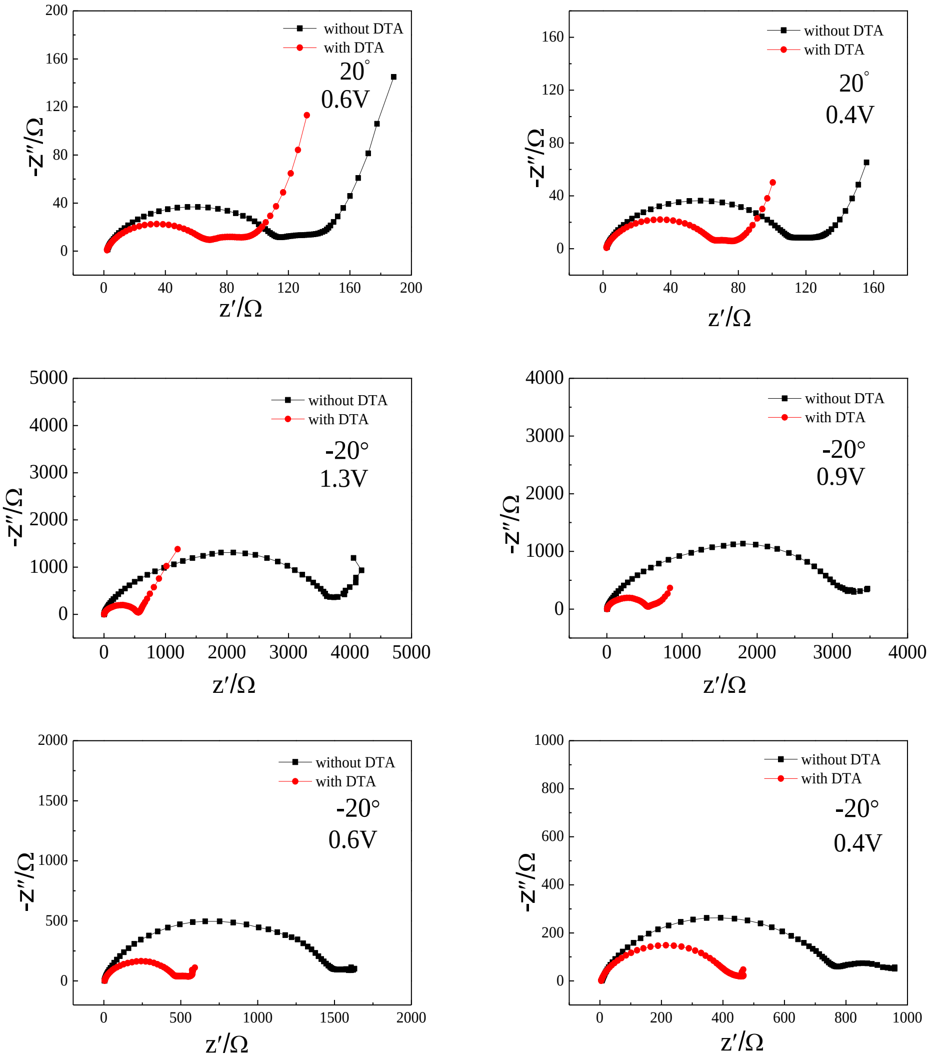

Figure 5. Nyquist diagrams of the graphite electrode in the first discharge process in the electrolyte without and with DTA at various potentials at 20°C and -20°C.

In order to further investigate why the electrochemical performance of graphite electrode in the electrolytes with DTA was improved, the EIS test was conducted. Figure 5 gives Nyquist plot of the graphite electrode in the first discharge process in the electrolyte with and without DTA at different potentials at 20°C and -20°C. Obviously, the EIS curves of graphite electrode in the electrolyte with and without DTA are similar at 20°C. When the potential is above 0.9V, the EIS of the graphite anode are composed of two parts: a high-frequency semicircle (HFS) and a low-frequency region oblique line. As the polarization potential decreases, the LFL gradually close to the Z′ axis, and formed another middle frequency semicircle (MFS) and a steep sloping line in the low frequency region (LFL). According to previous studies[18-21], the HFS is related the course of lithium ions passing through SEI film, the MFS is related to charge transfer process at the electrolyte-electrode interface while LFL is attributed to lithium ions solid-state diffusion within the graphite electrode [22-23].

At -20°C, the variation of EIS in the electrolyte with and without DTA is similar, which is consisted of three parts, that is, HFS, MFS and LFL. The HFS and MFS at -20°C is much larger than those at 20°C, indicating more dynamic impedance, which consistent with the results in Figure 4.

Moreover, at the same temperature, the semicircle with DTA is also much smaller than those without DTA, further proving that the DTA additive can reduce the dynamic impedance of lithium ion battery.

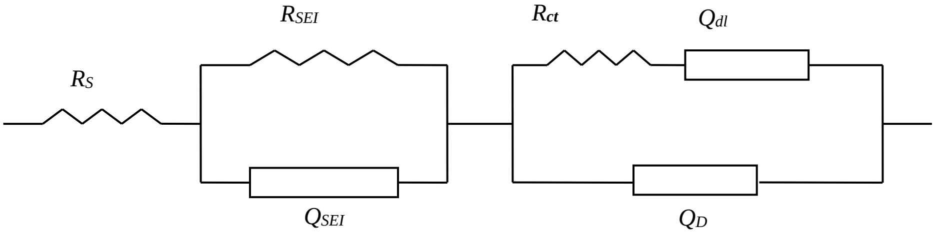

Figure 6. Equivalent circuit proposed for analysis of the graphite electrode

In order to discover the kinetic parameters and the implied mechanism, an equivalent circuit, as shown in Figure 6, was presented to fit Nyquist plots of the graphite electrode in electrolyte with and without DTA electrolyte in the first discharge process. In the equivalent circuit, R_s is associated with the ohmic resistance, while R_{SEI} and R_{ct} are resistances of the SEI film and the charge transfer reaction, respectively. The capacitance of the SEI film and the double layer are expressed by the constant phase elements (CPE) Q_{SEI} and Q_{dl}, respectively. The Q_D is related to diffusion impedance in the low-frequency region.

Table 1. The values of R_{SEI} at different potentials in the electrolyte with and without DTA at 20°C and -20°C

R_{SEI}/Ω P/V Condition		1.3	0.9	0.6	0.4
20°C	With DTA	52.14	65.03	66.15	52.14
	Without DTA	103.50	111.80	80.42	79.42
- 20°C	With DTA	529.60	523.50	444.00	141.10.
	Without DTA	3380.0	2943.00	1367.00	742.50

Table 1 gives the values of R_{SEI} at different potentials in the electrolyte with and without DTA at 20°C and -20°C. The values are obtained from fitting the experimental impedance spectra of the graphite electrode during the first discharge cycle by the equivalent circuit of Figure 6, and the fitting error is no more than 5%. Therefore, the equivalent circuit proposed in Figure 6 could satisfactorily describe the EIS data of the graphite anode at different temperature. From Table 1, it can be seen obviously that the resistance values of R_{SEI} at -20°C is much larger than those at 20°C, and the R_{SEI} with DTA is much smaller than that without DTA whether at high temperature of 20°C or low temperatures of -20°C. In our previous studies [17], the smaller the value of R_{SEI} is, the smaller the thickness of SEI film is, and so it is easier for lithium ion pass through the SEI film.

3.5. Characterization of graphite electrode surface

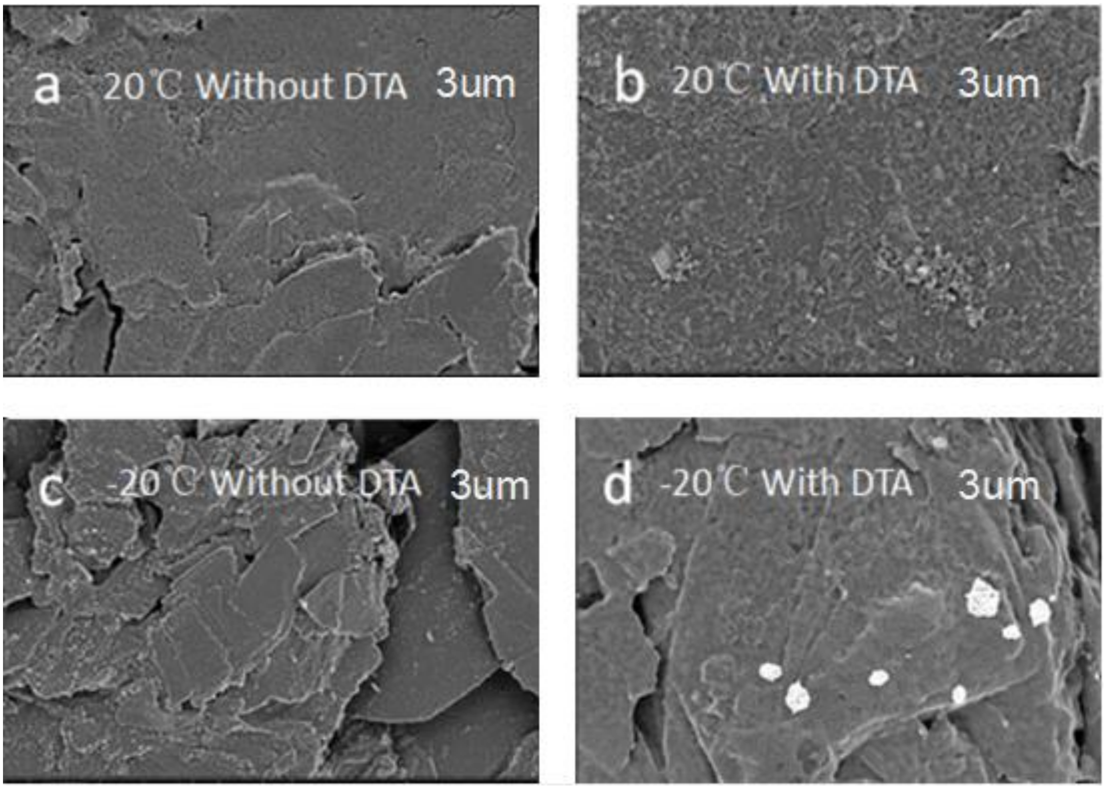

Figure 8. SEM images of the graphite electrode after 100 cycles in the electrolyte with and without DTA at 20℃and -20℃

In order to get more information about the improvement of electrochemical performance from the surface of the graphite electrode, SEM images of the graphite electrode after cycling in electrolyte with and without DTA are shown in Figure 8. It is found that in the electrolyte with DTA, a thin SEI film adhering to the graphite surface is compact and uniform. However in the electrolyte without DTA there are obvious cracks and uneven on the surface, which would lead to further reaction of the graphite with solution. It is indicated that the addition of DTA in the electrolyte successfully improves the morphology of SEI film on the graphite anode surface, and as a result leads to enhance the electrochemical performance of a half-cell with graphite as the negative electrode.

Meanwhile, the SEI film on the surface of the graphite electrode at -20℃ appear thicker than that at 20℃, corresponding to a larger impedance value, which is consistent with the above CV and the EIS data in Table 1.

3.6. XPS analysis of graphite electrode surface

To further investigate the effect of the DTA additive on the component of SEI, the XPS spectra of the graphite electrode cycled in the electrolyte with and without DTA at -20°C were determined. The XPS spectra of C1s, F1s and N1s were indicated in Figure 9.

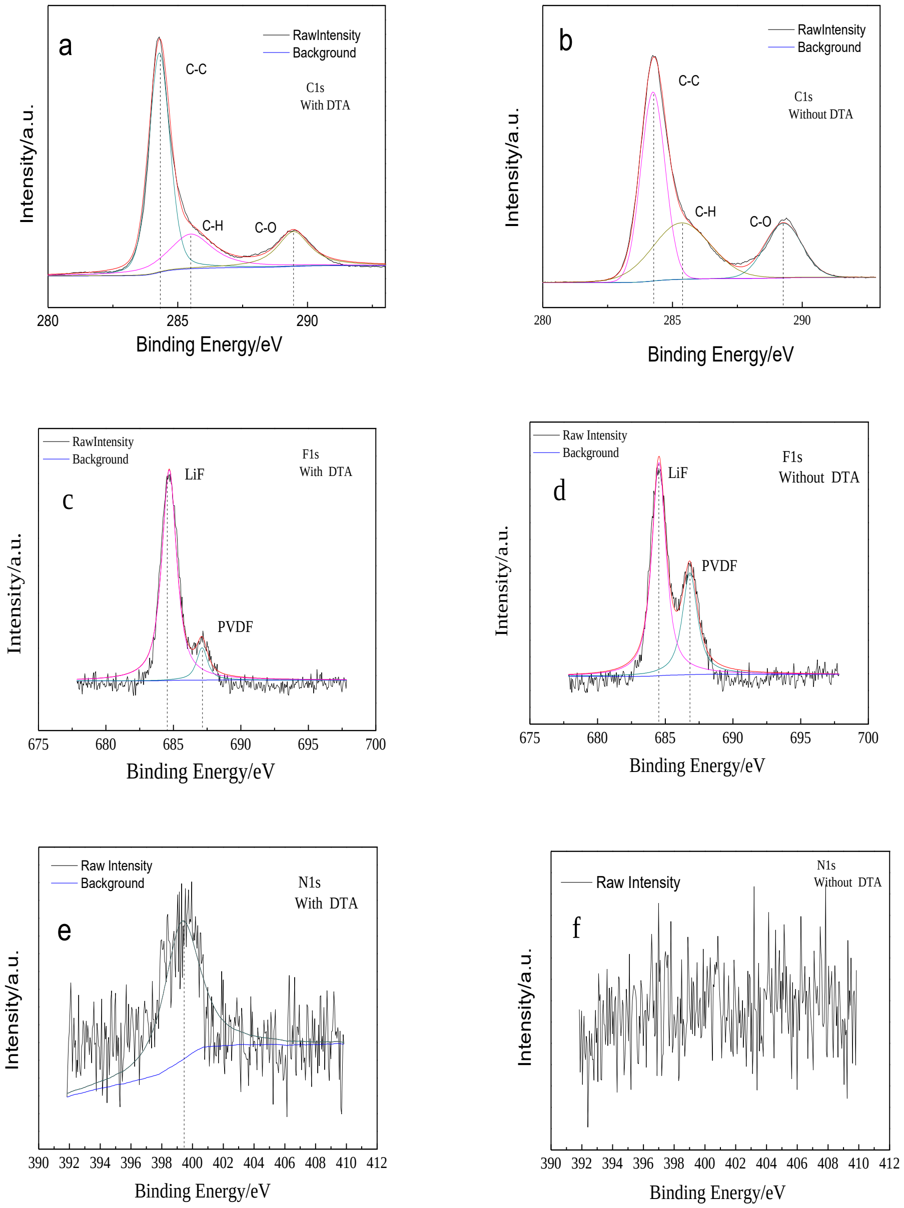

Figure 9. C1s, F1 and N1s XPS spectra of the graphite electrodes cycled after 100 cycles in the electrolyte with and without DTA at -20℃

From the C1s spectra, the peak at 284.6eV is attributed to the C-C bond [24], and the one at 285.5eV related to -CHO [25] and the one near 289.5eV related to the C-O bond and Li_2CO_3 [26]. Compared with without DTA, the area of peaks C-H and C-O bonds with DTA were remarkably smaller, indicating that the process of reductive decomposition of EC into $ROCO_2Li$ and Li_2CO_3 was weakened, which is consistent with the previously tested CV results.

From the F1s spectra, the peak at 687.8eV attributed to the C-F bond in the PVDF binder and the peak at 684.7eV is related to LiF [27]. It is clearly observed that the area of the LiF peak in the electrolyte with DTA is larger than the one without DTA, which indicates that DTA can enhance the amount of LiF on the electrode surface. LiF has high bonding ability and is not prone to decomposition, and has good insulation, low solubility in electrolyte, so it improves the stability of solid-liquid interface, therefore reducing the SEI film resistance [17].

The characteristic peak of N could not be detected for the graphite electrode in the electrolyte without DTA. However, the one of N around 399.3eV were clearly observed in Figure 9e with DTA, indicating that DTA is involved in the electrochemical reaction process during charge and discharge.

3.7. The reaction mechanism of DTA

In order to explain the reaction mechanism of DTA additive, the reaction occurring on the surface of SEI in the electrolyte with and without DTA is given in Figure 10.

The electrolyte lithium salt $LiPF_6$ would have the following decompose reaction during charge and discharge of the battery due to auto catalytic.

$$LiPF_6 \rightarrow PF_5 + LiF \qquad (5)$$

Then PF_5 reacts with most SEI components such as Li_2CO_3, RCO_2Li and $ROCO_2Li$, for example [7].

$$Li_2CO_3 + PF_5 \rightarrow POF_3 + 2LiF + CO_2 \qquad (6)$$

The CO_2 product would lead to gas expansion inside the battery, so the electrochemical performance of the graphite electrode would deteriorate.

The DTA additive is a donor of electron pairs because of its nitrogen nucleus with a lone pair of electrons, and PF_5 becomes a receptor for electron pair because of its electron defect type, and the both would combine to form a weak composite [7], thereby reducing the reactivity of PF_5 and weakening the occurrence of Formula 6. Meanwhile, DTA provides F^- groups, which can form an appropriate amount of LiF, improving the stability of the SEI film [17].

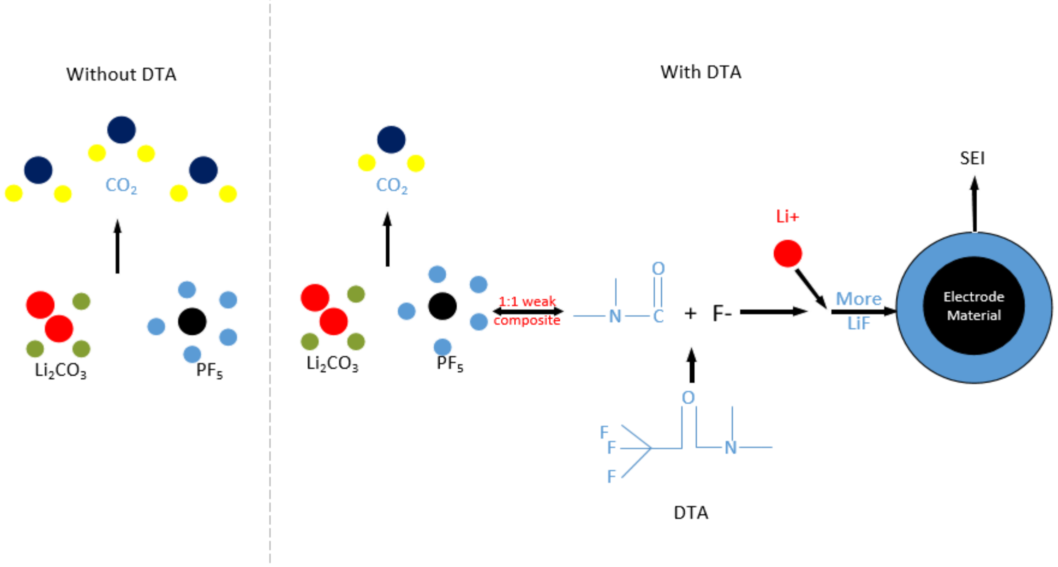

Figure 10. The reaction occurring on the surface of the SEI in the electrolyte with and without DTA

4. CONCLUSION

The results of this work indicates that adding 2% DTA to the electrolyte can enhance the ionic conductivity and improve the electrochemical performance of the graphite electrode at room temperature of 20°C and low temperature of -20°C, and the EIS demonstrates the SEI film formed with DTA as an electrolyte additive has a smaller resistance at -20°C. The improved performance can be attributed to a richer LiF composition in the SEI film on the interfaces between the electrolyte and DTA attenuates the reaction of the PF_5 with Li_2CO_3.

ACKNOWLEDGEMENT

This work was supported by National Natural Science Foundation of China (U1730136) and the Fundamental Research Funds for the Central Universities (2017XKQY062).

References

1. K. M. Kim, Y. Lee, J. H. Park, J. M. Ko, *Etri J.,* 2(2016)252-259
2. Z. Lei, Y. Zhang, X. Lei, *Int. J. Heat Mass Transfer*, 121(2018)275-281
3. A. Wang, S. Kadam, H. Li, S. Shi, Y. Qi, *Comp. Mater.*, 4(2018) 15
4. S. Kim, T. Han, J. Jeong, H. Lee, M. H. Ryou, Y. M. Lee, *Electrochim. Acta,* 241(2017)553-559
5. S. Moon, H. Park, G. Yoon, M. H. Lee, K. Y. Park, K. Kang, *Chem. Mater.,* 29(2017)9182-9191
6. R. Schmuch, R. Wagner, H. Gerhard, T. Placke, M. Winter, *Nat. Energy*, 3(2018) 267-278
7. N. L. Hamidah, G. Nugroho, F. Wang, *Ionics,* 22(2016) 33-41
8. M. T. F. Rodrigues, G. Babu, H. Gullapalli, K. Kalaga, F. N. Sayed, K. Kato, J. Joyner, P. M. Ajayan, *Nat. Energy,* 2(2017)17108
9. Y. Cui, Y. Pu,Y. Hao, Q. Zhang, *Russ. J. Electrochem.,* 51(2015) 119-124.
10. R. Miao, J. Yang, Z. Xu, *Sci. Rep.*, 6(2016):21771
11. L. Xia, L.Yu, D. Hu, Z. G. Chen, *Acta Chim. Sinica,* 75(2017) 1183-1195.
12. S. Chen, Z. Wang, H. Zhao, H. Qiao, H. Luan, L. Chen, *J. Power Sources* 187 (2009) 229-232.
13. Q. Wang, P. Ping, X. Zhao, G. Chu, J. Sun, C. Chen, *J. Power Sources*, 208(2012) 210-224.
14. X. L. Xu, S. X. Deng, H. Wang, J. B. Liu, H. Yan, *Nano-Micro Lett.*, 9(2017) 22
15. F. J. Bian, Z. R. Zhang, Y. Yang, *J. Electrochem.*,19(2013) 355-360.
16. Y. Wang, S. Nakamura, M. Ue, *J. Am. Chem. Soc.*, 123(2001) 11708-11718.
17. L. Liao, X. Cheng, Y. Ma, P Zuo, W. Fang, G. Yin,Y. Gao, *Electrochim. Acta*, 87 (2013) 466-472
18. C. Chae, H. J. Noh, J. K. Lee, B. Scrosati, Y. K. Sun, *Adv. Funct. Mater.*, 24(2014) 3036-3042.
19. J. Ryu, T. Chen, T. Bok, G. Song, J. Ma, C. Hwang, L. Luo, H. K. Song, J. Cho, C. Wang, S. Zhang, S. Park, *Nat. Commun.*, 9(2018) 2924
20. J. Li, Y. Qian, L. Wang, X. He, *Mat.*, 11(2018) 134
21. W. C. Choi, D. Byun, J. K. Lee, B. W. Cho, *Electrochim. Acta,* 50(2004) 523-529
22. M. Petzl, M. Kasper, M. A. Danzer, *J. Power Sources,* 275(2015)799-807
23. F. Dinkelacker, P. Marzak, J. Yun, Y. Liang, A. S. Bandarenka, *ACS Appl. Mater. Inter.,* 10(2018)14063-14069.
24. M. Holzapfel, A. Martinent, F. Alloin, B. L.Gorrec, R.Yazami, C. Montella, *J. Electroanal. Chem.,* 546(2003) 41-50
25. X. Li, Y. Qian, T. Liu, F. Cao, Z. Zang, X. Sun, S. Sun, Q. Niu, J. Wu, *J. Mater. Sci.*, 53(2018) 1-13.
26. Z. Cai, Y. Liu, J. Zhao, L. Li, Y. Zhang, J. Zhang, *J. Power Sources*, 202(2012) 341-346.
27. B. Chen, L. Ben, H. Yu,Y. Chen, X. Huang, *ACS Appl. Mater. Inter.,* 10(2018)1550-559